The Journal of Immunology
RESEARCH ARTICLE | MARCH 01 2010

Anti-Programmed Cell Death 1 Antibody Reduces $CD4^+PD\text{-}1^+$ T Cells and Relieves the Lupus-Like Nephritis of NZB/W F1 Mice FREE

Shimpei Kasagi; ... et. al

J Immunol (2010) 184 (5): 2337–2347.
https://doi.org/10.4049/jimmunol.0901652

Anti-Programmed Cell Death 1 Antibody Reduces $CD4^+PD\text{-}1^+$ T Cells and Relieves the Lupus-Like Nephritis of NZB/W F1 Mice

Shimpei Kasagi,* Seiji Kawano,* Taku Okazaki,† Tasuku Honjo,‡ Akio Morinobu,* Saori Hatachi,§ Kenichiro Shimatani,¶ Yoshimasa Tanaka,¶ Nagahiro Minato,¶ and Shunichi Kumagai*

Programmed cell death 1 (PD-1) is an immunosuppressive receptor that transduces an inhibitory signal into activated T cells. Although a single nucleotide polymorphism in the gene for PD-1 is associated with susceptibility to systemic lupus erythematosus, the role of PD-1 in systemic lupus erythematosus is still not well understood. In this study, we used NZB/W F1 mice, a model of lupus-like nephritis, to examine the function of PD-1 and its ligands. PD-1 was predominantly expressed on $CD4^+$ T cells that infiltrated the kidney, and $CD4^+PD\text{-}1^{high}$ T cells produced higher levels of IFN-γ than $CD4^+PD\text{-}1^{low}$ or $CD4^+PD\text{-}1^-$ T cells. Stimulation with PMA/ionomycin caused splenic $CD4^+PD\text{-}1^+$ T cells to secrete high levels of IFN-γ, IL-10, low levels of TNF-α, faint levels of IL-2, IL-21, and no IL-4, IL-17. In vivo anti–PD-1 mAb treatment reduced the number of $CD4^+PD\text{-}1^+$ T cells in the kidney of NZB/W F1 mice and significantly reduced their mortality rate ($p = 0.03$). Conversely, blocking PD-L1 using an anti–PD-L1 mAb increased the number of $CD4^+PD\text{-}1^+$ T cells in the kidney, enhanced serum IFN-γ, IL-10, and IgG2a ds-DNA–Ab levels, accelerated the nephritis, and increased the mortality rate. We conclude that $CD4^+PD\text{-}1^{high}$ T cells are dysregulated IFN-γ–producing, proinflammatory cells in NZB/W F1 mice. ***The Journal of Immunology*****, 2010, 184: 2337–2347.**

Systemic lupus erythematosus (SLE) is an autoimmune disease that affects multiple organs and body systems. The immune system abnormalities caused by SLE are complex and involve pathogenic autoantibody production driven by autoimmune Th cells (1). NZB/W F1 mice spontaneously develop a syndrome resembling human SLE (2) and are frequently used as surrogates for studying this disease. As in humans, Ag-specific Th cells in NZB/W F1 mice mediate the inflammatory damage and the development of severe immune complex-related glomerulonephritis. The dysregulation of Th cells in NZB/W F1 mice also plays a major role in polyclonal B cell activation and autoantibody production (2). Under normal conditions, the clonal deletion of activated T cells mediated by apoptosis or anergy contributes to the maintenance of immunologic self-tolerance; broken self-tolerance leads to the development of SLE (3). In this context, inhibitory signals delivered through costimulatory pathways to activated T cells are essential for the recovery of self-tolerance in SLE (4).

Programmed cell death 1 (PD-1) is an inhibitory costimulatory receptor whose expression in a thymic T cell line is enhanced by apoptotic stimuli (5). The protein consists of a single extracellular IgV-like domain, a transmembrane domain, and an intracellular tail that contains an immunoreceptor tyrosine-based switch motif and an ITIM. In vitro experiments have shown that the tyrosine residue located within the immunoreceptor tyrosine-based switch motif is phosphorylated on Ag stimulation, after which it recruits the protein tyrosine phosphatase Src homology region 2-containing protein tyrosine phosphatase-2, which leads to the dephosphorylation, and hence the inhibition, of effector molecules that are activated by TCR or B cell receptor signaling (6). Thus, the suppression of PD-1 of both TCR-mediated and CD28-mediated signaling alters the threshold for T cell activation and cytokine production (7).

PD-1 belongs to the CD28 Ig superfamily and shares 23% amino acid sequence identity with CTL-associated Ag 4 (CTLA-4) (6). Its expression is induced on activated T cells and B cells; on interaction with its ligands, PD-L1 and PD-L2, it transduces an inhibitory signal to activated T cells (8). PD-L1 is expressed on a wide variety of nonhematopoietic cell types, including vascular endothelial cells, pancreatic islet cells, astrocytes, and keratinocytes, and on lymphoid organ cells, whereas PD-L2 is expressed only on hematopoietic APCs (9, 10). PD-1 and its ligands play important roles in the regulation of T cell activation and in the maintenance of T cell tolerance (9, 11), as evidenced by the lupus-like glomerulonephritis with glomerular deposition of IgG and C3 developed by PD-1 knockout mice on the C57BL/6 background (12), and by the cardiomyopathy accompanied by the production of autoantibodies against cardiac troponin I the develops in PD-1 knockout mice on the BALB/c background (13, 14). In humans, a single nucleotide polymorphism in intron 4 of the PD-1 gene (*PD1.3A*) is associated with the development of SLE or lupus nephritis (in Europeans and Mexicans) (15, 16).

*Department of Clinical Pathology and Immunology, Kobe University Graduate School of Medicine, Kobe, Hyogo; †Division of Immune Regulation, Institute for Genome Research, University of Tokushima, Tokushima; §Department of Rheumatology, Kitano Hospital, Osaka; and ‡Department of Immunology and Genetic Medicine and ¶Department of Immunology and Cell Biology, Graduate School of Medicine, Kyoto University, Kyoto, Japan

Received for publication May 27, 2009. Accepted for publication December 29, 2009.

This work was supported in part by Grant-in-Aid for Scientific Research 17591042 and 19591167 (to S. Kawano) from the Japan Society for the Promotion of Science.

Address correspondence and reprint requests to Prof. Shunichi Kumagai, Department of Clinical Pathology and Immunology, Kobe University Graduate School of Medicine, 7-5-2 Kusunoki-Cho, Chuo-Ku, Kobe, Hyogo, 650-0017 Japan. E-mail address: kumagais@kobe-u.ac.jp

The online version of this article contains supplemental material.

Abbreviations used in this paper: BTLA, B and T lymphocyte attenuator; CDC, complement-dependent cytotoxicity; EAE, experimental allergic encephalitis; FoxP3, forehead box P3; PAS, periodic acid Schiff; PD-1, programmed cell death 1; PFA, paraformaldehyde; PI, propidium iodide; SLE, systemic lupus erythematosus; Treg, T regulatory; Tr1, type 1 Treg.

www.jimmunol.org/cgi/doi/10.4049/jimmunol.0901652

Several reports, including ours on the synovitis of rheumatoid arthritis and the sialoadenitis of Sjögren's syndrome, show that PD-1$^+$ T cells accumulate at sites of inflammation in several human autoimmune diseases (17–20). Although the contribution of PD-1 to the pathogenesis of human SLE was first noted in 1999, the biological function of PD-1 in SLE remains a mystery. In this study, we investigated the role played by PD-1 and its ligands, PD-L1 and PD-L2, in the development of lupus-like nephritis in NZB/W F1 mice. We examined the in vivo effects of anti–PD-1 and anti–PD-L1 mAbs in NZB/W F1 mice and the distribution of PD-1, PD-L1, PD-L2, and T cells with the CD4$^+$PD-1$^+$ phenotype. We found that an anti–PD-1 Ab was effective for treating the lupus-like nephritis of NZB/W F1 mice and that CD4$^+$PD-1$^+$ T cells played a key role in the progression of lupus nephritis in this model.

Materials and Methods

Animals

Female NZB mice and male NZW mice were obtained from SLC (Sizuoka, Japan), and kept in a specific pathogen-free environment at the animal experiment facility at the Kobe University Graduate School of Medicine. Lupus-prone NZB/W F1 mice were obtained by crossing the NZB and NZW mice. All the mice were cared for in accordance with the institutional guidelines for animal experiments.

Abs and treatment protocol

Twenty female NZB/W F1 mice at 16–17 wk of age were randomly assigned to a control or treatment group (n = 10 per group). They then received i.p. injections of isotype control Ab (hamster IgG) or anti–PD-1 mAb (clone: J43, hamster IgG) (250 μg/body) (21) three times per week for 10 wk. Anti–PD-L1 mAb (clone: 111A, rat IgG2a) (250 μg/body) (22) or isotype control Ab (rat IgG) was administered by the same method. The anti–PD-1 and anti–PD-L1 mAbs were harvested and purified from hamster and murine ascites, respectively, using a standard method for generating mAbs. Isotype control Abs were isolated and purified from rat or Armenian hamster serum by passage over a Protein G affinity purification column. To monitor the development of nephritis, proteinurea was assessed using a Multistix PRO (Bayer Diagnostics, Medfield, MA); severe proteinurea was defined as >300 mg/dl. Sera were collected monthly from 16- to 24-wk-old mice and stored at −80°C.

Complement-dependent cytotoxicity assay

The complement-dependent cytotoxicity (CDC) assay was performed using RHBP medium [RPMI 1640 supplemented with 0.1% BSA, 20 mM HEPES (pH 7.2–7.4), 100 IU/ml penicillin, and 100 μg/ml streptomycin]. One hundred microliters RHBP medium containing 10^5 IIA1.6 cells (23), and 100 μl RHBP medium containing various concentrations of anti–PD-1 mAb (J43) were added to flat-bottomed 96-well tissue culture plates and incubated for 1 h at 4°C. After centrifugation, the cells were resuspended in RHBP medium containing a 1/20 vol fresh rabbit serum (Low-Tox-M Rabbit complement) (Cedarlane, Burlington, Ontario, Canada) as a complement source, and incubated for 2 h at 37°C, 5% CO_2 to facilitate complement-mediated cell lysis. The cell lysis was measured by the trypan blue exclusion assay, or by propidium iodide (PI) staining using flow cytometry.

Histopathology

Kidneys were harvested when the mice were sacrificed and immediately immersed in 4% paraformaldehyde (PFA) 1 h or embedded in OCT compound and frozen in liquid nitrogen. The kidney specimens immersed in 4% PFA were embedded in paraffin blocks after overnight fixation, and 5-μm sections were cut and stained with periodic acid Schiff (PAS). The frozen tissues stored in liquid nitrogen were cut into 5-μm cryosections, fixed in Cytofix/cytoperm (BD Biosciences, San Jose, CA), and stained with polyclonal Abs against PD-1, PD-L1, and PD-L2 (R&D Systems, Minneapolis, MN); CD80 (eBioscience, San Diego, CA); CD4, CD8a, CD31, and CD45RB220 (BD Biosciences); and type IV collagen (Chemicon, Temecula, CA). FITC- or PE-conjugated donkey anti-rat or anti-goat IgG, or PE-conjugated donkey anti-rabbit IgG were purchased from Jackson ImmunoResearch Laboratories (West Grove, PA). The sections were stained with FITC-conjugated goat anti-mouse IgG, IgG1, IgG2a, IgG3, or C3 Abs (Cappel Laboratories, West Chester, PA), and the fluorescence from the IgG and C3 deposits within glomeruli were analyzed using a fluorescence microscope. The glomerular pathology was assessed in 20 glomeruli per kidney in PAS-stained cross-sections, as described previously by Nozaki et al. (24). The tubular pathology was assessed from the percentage of tubules showing damage (dilatation, atrophy, or necrosis) among 200 tubules in randomly chosen fields. The renal pathology was assessed by two investigators.

Flow cytometry

The spleen and kidneys from sacrificed mice were passed through a 70-μm cell strainer (BD Biosciences), and the single-cell suspension was washed twice with PBS containing 0.5% BSA (PBS/BSA). Erythrocytes were eliminated using ACK lysis buffer (Nalgene, Rochester, NY) containing 0.83% NH_4Cl, and the cells were then washed again with PBS/BSA. The cells were then stained with FITC-conjugated anti-ICOS, -CD8a, -CD45RB220, -CD44, -CD62L, -CD69, -CD80, -CD86, –CTLA-4, –PD-1 (J43), and -forehead box P3 (FoxP3) mAbs; PE-conjugated anti–PD-1(J43 and RMP1-30) and -B and T lymphocyte attenuator (BTLA) mAbs (eBioscience); peridinin chlorophyll α protein (PerCP)-conjugated anti-CD4 mAb; and allophycocyanin-conjugated anti-CD25 mAb (BD Biosciences). The cells were then fixed with 1% PFA for 20 min at 4°C and analyzed in a FACScalibur (BD Biosciences). Two-color flow cytometry was performed to examine the percentage of PD-1$^+$ lymphocytes in NZB, NZW, NZB/W F1, and BALB/c mice. Four-color flow cytometry was performed to examine the percentage of CD4$^+$PD-1$^+$ or CD4$^+$PD-1$^-$ T cells expressing CD25, CD44, CD62L, CD69, CD80, CD86, CTLA-4, BTLA, ICOS, or intracellular FoxP3.

Intracellular cytokine assay

CD4$^+$ T cells were purified by MACS positive selection (Miltenyi Biotec, Auburn, CA), and then were activated with PMA/ionomycin (final concentrations: PMA 10 μg/ml, ionomycin 1 μg/ml) and incubated for 4 h at 37°C in RPMI medium containing 10% FBS (Life Technologies, Rockville, MD) and brefeldin A (final concentration: 10 μg/ml). The cells were then stained with FITC-conjugated anti–PD-1 mAb and PerCP-conjugated anti-CD4 mAb, fixed with Cytofix/cytoperm (BD Biosciences) for 20 min at 4°C, and washed twice with PBS/BSA containing 0.5% saponin. To detect intracellular cytokines, the cells were incubated for 30 min at 4°C with PE-conjugated anti–IFN-γ, IL-2, IL-4, IL-17, and TNF-α mAbs, and allophycocyanin-conjugated anti–IL-10 and IFN-γ mAbs (eBioscience). For the measurement of intracellular IL-21, cells were incubated with IL-21R/Fc chimera (R&D Systems) for 30 min at 4°C. Cells were then washed three times and stained with PE-conjugated affinity-purified F(ab′)$_2$ fragment of goat anti-human Fcγ Ab (Jackson ImmunoResearch Laboratories) for 30 min at 4°C. A four-color flow analysis was then performed to examine the percentage of CD4$^+$PD-1$^+$ or CD4$^+$PD-1$^-$ T cells that were producing these cytokines.

Proliferation assay and ELISA for cytokines and autoantibodies

CD4$^+$ T cells purified by MACS positive selection were stained with an allophycocyanin-conjugated PD-1 mAb. The CD4$^+$PD-1$^+$ and CD4$^+$PD-1$^-$ T cells were then sorted using a FACS Vantage SE (BD Biosciences). Purity >95% was consistently obtained for the CD4$^+$PD-1$^+$ and CD4$^+$PD-1$^-$ T-cell fractions. Both cell types were then incubated with plate-bound anti-CD3 mAb (1 μg/ml/well) for 3 d, alone or in the presence of soluble anti-CD28 mAb (10 μg/ml) (BD Biosciences) or recombinant human IL-2 (hIL-2, 100 U/ml) (BD Biosciences). For the final 24 h of incubation, 1 Ci ^{3}H-thymidine was added to each well, and the incorporation of ^{3}H-thymidine was determined using a liquid scintillation counter.

For the measurements of IFN-γ and IL-2 production from CD25$^-$ PD-1$^+$ and CD25$^-$ PD-1$^-$ T cells, CD4$^+$ T cells were stained with an FITC-conjugated anti-CD4 mAb, PE-conjugated anti–PD-1 mAb, allophycocyanin-conjugated anti-CD25 mAbs, and 7-aminoactinomycin D. The CD25$^-$ PD-1$^+$ and CD25$^-$ PD-1$^-$ T cells were then separately sorted. Purity >95% was consistently obtained for both fractions. Each cell type (10^5 cells/well) was then incubated with plate-bound anti-CD3 mAb (1 μg/ml/well) for 8 h, alone or in the presence of soluble anti-CD28 mAb (10 μg/ml) (BD Biosciences). The supernatants were collected, and the levels of serum IFN-γ and IL-2 were measured by ELISA with BD optEIA ELISA kits (BD Biosciences). For the measurement of IgG anti–ds-DNA Ab, each cell type (10^5 cells/well) was incubated for 12 h with plate-bound anti-CD3 mAb (1 μg/ml/well), soluble anti-CD28 mAb (10 μg/ml) (BD Biosciences), and B220$^+$ cells (10^4 cells/well) that were harvested from the spleen of 32-wk-old NZB/W F1 mice and purified by MACS positive selection. Supernatants were collected, and then the level of IgG anti–ds-DNA Ab was measured using a mouse IgG anti–ds-DNA ELISA kit (Sibayagi, Gunma, Japan). The

levels of serum IL-4, IL-6, IL-10, IFN-γ, and TNF-α were measured with BD optEIA ELISA kits; the level of serum TGF-β was measured with a Duoset ELISA development kit (R&D Systems). Each ELISA was performed in triplicate.

Statistical analysis

All data are presented as the mean ± SD. Groups of data were compared using a two-tailed Student *t* test or nonparametric Mann-Whitney signed rank test. Kaplan-Mayer survival graphs were constructed, and a log-rank comparison or Fisher exact test of the groups was used to calculate *p* values. Values of $p < 0.05$ were considered significant.

Results

Enhanced PD-1 and PD-L1 expression in the kidneys of NZB/W F1 mice

To investigate whether interactions between PD-1 and its ligands, PD-L1 and PD-L2, are involved in the pathogenesis of NZB/W F1 mice, we first examined the renal expression of PD-1 and PD-L1/L2 by indirect immunofluorescence. We detected none of the three molecules in the prenephritic kidneys of 20-wk-old NZB/W F1 mice. In the nephritic kidneys of 36-wk-old mice, however, PD-L1 was expressed in the glomeruli, and both PD-1 and PD-L2 were expressed in the periglomerular regions (Fig. 1*A*). The infiltrating leukocytes in the nephritic kidneys consisted mainly of CD45RB220-positive ($B220^+$) B and $CD4^+$ T cells and, to a small extent, $CD8^+$ T cells (Fig. 1*B*). PD-1 was mainly expressed on the $CD4^+$ T cells. PD-L1 was strongly expressed on glomerular endothelial cells, which were marked by CD31, and on urinary tube epithelial cells, which were marked by type IV collagen. In contrast, PD-L1 was not strongly expressed on glomerular parenchymal cells (Fig. 1*C*,1*D*). The infiltrating leukocytes were mostly $PD\text{-}L1^+$, and some were $PD\text{-}1^+$ and $CD80^+$, but very few were $PD\text{-}L2^+$.

Increased percentage of $CD4^+PD\text{-}1^+$ T cells in the spleen and kidneys of NZB/W F1 mice

Table I shows the phenotypes of splenic cells from NZB, NZW, NZB/W F1, and BALB/c mice, determined by flow cytometry. The percentage of $CD4^+PD\text{-}1^+$ T cells among the splenic

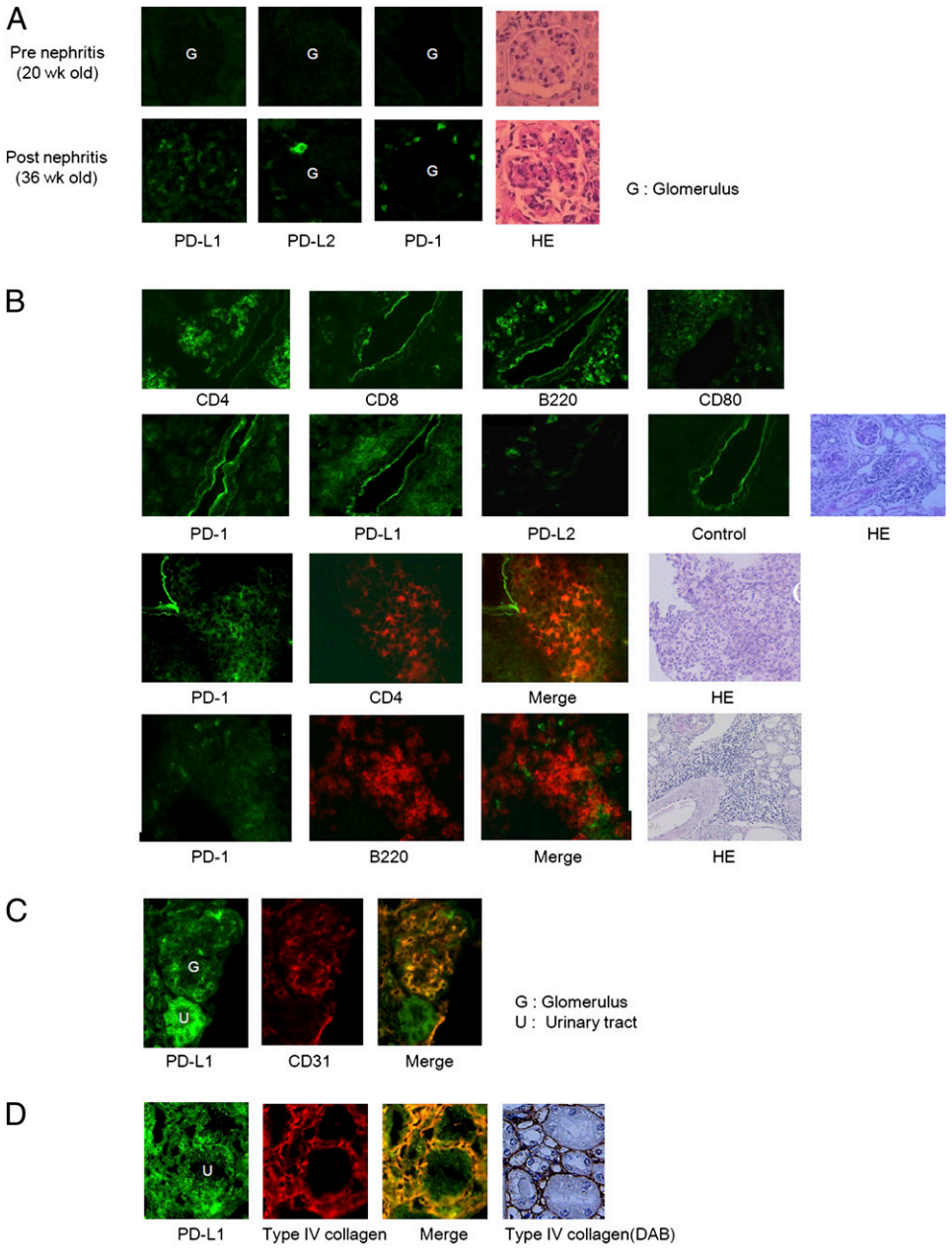

FIGURE 1. PD-1 and PD-L expression in the kidneys of NZB/W F1 mice. *A*, PD-1 and PD-L1 expression in the glomeruli of NZB/W F1 mice at 20 and 36 wks of age. *B*, PD-1, PD-L1, PD-L2, CD4, CD8, CD45RB220, and CD80 expression on the perivascular infiltrating cells in the nephritic kidney (NZB/W F1, 36 wk old). Double staining of PD-1 (green) and CD4 (red) or CD45RB220 (red) is also shown. *C*, Double staining of PD-L1 (FITC, green) and CD31 (PE, red) in glomeruli (NZB/W F1, 36 wk old). *D*, Double staining of PD-L1 (green) and type IV collagen (red), and DAB (3, 3′-diaminobenzidine) staining in the urinary tract (NZB/W F1, 36 wk old). Each panel contains consecutive frozen sections of the kidney. Original magnification ×200.

Table I. *Phenotypic analysis of splenic cells from NZB (female), NZW (male), NZB/W F1 (female), and BALB/c (female) mice*

Spleen Cells	NZB[a]	NZW[a]	NZB/WF1[a]	Balb/c[a]
$CD4^+$ T cells (%)				
Young (16 wk)	26.8 ± 2.127	9 ± 4.6	25.0 ± 3.2	21.1 ± 5.6
Old (36 wk)	23.0 ± 6.6	24.9 ± 8.9	27.0 ± 3.3	26.4 ± 9.3
$CD8^+$ T cells (%)				
Young (16 wk)	7.5 ± 2.1	12.7 ± 3.4	13.6 ± 4.6	13.3 ± 4.3
Old (36 wk)	8.1 ± 2.9	10.4 ± 4.1	11.8 ± 7.0	18.1 ± 16.5
CD45RB220 $(B220)^+$ (%)				
Young (16 wk)	44.0 ± 7.6	45.0 ± 9.8	46.7 ± 7.6	38.4 ± 4.8
Old (36 wk)	43.8 ± 14.8	46.2 ± 8.1	47.3 ± 5.7	44.6 ± 9.0
$CD4^+PD\text{-}1^+$ (%)				
Young (16 wk)	6.3 ± 1.7*	6.8 ± 1.3	8.0 ± 1.4*	8.8 ± 1.7
Old (36 wk)	19.5 ± 8.1*	8.5 ± 1.3	20.5 ± 3.5	10.8 ± 2.7
$CD8^+PD\text{-}1^+$ (%)				
Young (16 wk)	8.8 ± 3.0	12.0 ± 2.2	7.2 ± 4.3	7.0 ± 3.0
Old (36 wk)	5.0 ± 2.3	10.8 ± 2.2	8.8 ± 3.4	11.2 ± 2.7
$B220^+PD\text{-}1^+$ (%)				
Young (16 wk)	6.5 ± 2.1*	6.3 ± 1.9	2.2 ± 1.2	1.5 ± 2.0
Old (36 wk)	15.5 ± 5.7*	7.0 ± 2.5	2.4 ± 0.7	1.1 ± 0.7

Phenotypes of splenic cells from 16-wk-old or 36-wk-old NZB (female), NZW (male), NZB/W F1 (female), and BALB/c (female) mice ($n = 3$, at 16 or 36-wk-old) are shown.

[a] $n = 3$.

*$p < 0.05$.

lymphocytes did not show much difference among the NZB, NZW, NZB/W F1, and BALB/c mice at 16 wk of age. However, when 16- and 36-wk-old mice were compared, the percentage of $CD4^+PD\text{-}1^+$ T cells among the splenic lymphocytes was significantly higher in the 36-wk-old than the 16-wk-old NZB and NZB/W mice ($p < 0.05$) but not in the NZW and BALB/c mice. No significant differences in the percentage of $CD8^+PD\text{-}1^+$ T cells were seen among any of the strains. By contrast, we observed an increased percentage of $B220^+PD\text{-}1^+$ cells in the female NZB mice, but not the other strains, including NZB/W F1. Examination of the NZB/W F1 mice at 36 wk of age showed that a high proportion of the $CD4^+$ T cells in the kidneys and spleen were $PD\text{-}1^+$ (Fig. 2*A*).

$CD4^+PD\text{-}1^{high}$ T cells produce high levels of IFN-γ

We next used flow cytometry to investigate the phenotype and function of the splenic $CD4^+PD\text{-}1^+$ T cells in 16-wk-old, prenephritic NZB/W F1 mice. Intracellular cytokine staining showed that splenic $CD4^+PD\text{-}1^+$ T cells produced high levels of IFN-γ, IL-10, low levels of TNF-α, faint levels of IL-2, IL-21, and no IL-4, IL-17. By contrast, $CD4^+PD\text{-}1^-$ T cells produced only TNF-α and IL-10 (Fig. 2*B*). Notably, when the $CD4^+PD\text{-}1^+$ T cells were separated into $PD\text{-}1^{high}$ and $PD\text{-}1^{low}$ T cells, the $CD4^+PD\text{-}1^{high}$ T cells produced much higher levels of IFN-γ than the $CD4^+$ $PD\text{-}1^{low}$ T cells, but their production of IL-10 did not differ significantly. Accordingly, we found that the $CD4^+PD\text{-}1^+$ T cells in the spleen and kidneys of mice at the nephritic stage secreted high levels of IFN-γ (Fig. 2*C*). We further analyzed the $CD4^+PD\text{-}1^+$ T cells for IFN-γ/IL-10 production in relation to their CD25 positivity. We found that IFN-γ and IL-10 were mostly produced by the $CD25^+PD\text{-}1^+$ and $CD25^-PD\text{-}1^+$cells, and not by $PD\text{-}1^-$ cells (Fig. 2*D*). IFN-γ was predominantly produced by $CD25^-$ $PD\text{-}1^+$ cells (Fig. 2*D*), and >80% of the $PD\text{-}1^+$ cells were $CD25^-$ (Supplemental Fig. 1). The $CD25^-PD\text{-}1^+$ cells produced much higher levels of IFN-γ and IL-2 than the $CD25^-PD\text{-}1^-$ T cells, when they were stimulated with anti-CD3/CD28 mAbs (Fig. 2*E*). A sizable percentage of $CD25^+PD\text{-}1^+$ cells produced IL-10 (Fig. 2*D*), and more than half of the $CD25^+PD\text{-}1^+$ cells were also positive for intracellular FoxP3 (Supplemental Fig. 1). These IL-10-producing $CD4^+CD25^+FoxP3^+$ T cells resembled regulatory T cells (Treg) cells. In contrast, a considerable portion of the IL-10–producing $CD25^-PD\text{-}1^{high}$ T cells were $CD45RB^{low}$, resembling type 1 Treg (Tr1) cells (unpublished observations). We therefore concluded that the $CD4^+PD\text{-}1^+$ T cells are heterogeneous and include IFN-γ–producing $PD\text{-}1^{high}$ cells and possibly other immuno-Treg cells.

$CD4^+PD\text{-}1^{high}$ T cells show an effector/memory phenotype and poor proliferation capacity

$CD4^+PD\text{-}1^+$ T cells exhibited the activated T cell phenotype, in contrast to $CD4^+PD\text{-}1^-$ T cells (Table II). Three B7 family molecules, CD80, CD86, and ICOS, were predominantly expressed on the $CD4^+PD\text{-}1^+$ T cells, which also expressed immunoregulatory costimulatory molecules, such as CTLA-4 and BTLA. FoxP3-positive cells constituted only a minor population (4.4%) of the $CD4^+PD\text{-}1^+$ T cells. In addition, the majority of $CD4^+PD\text{-}1^+$ T cells exhibited the $CD62L^{low}CD69^{high}CD44^{high}$ effector/memory phenotype, and the majority of the $CD4^+PD\text{-}1^-$ T cells exhibited the $CD62L^{high}CD69^{low}CD44^{low}$ naive phenotype (Supplemental Fig. 1). Collectively, the effector/memory markers, the B7 family molecules, and the immunoregulatory costimulatory molecules were concomitantly expressed on $CD4^+PD\text{-}1^{high}$ T cells, and their expression on $PD\text{-}1^{high}$ cells was greater than on $PD\text{-}1^{low}$ cells. By contrast, $CD4^+PD\text{-}1^-$ T cells expressed none of these costimulatory molecules.

The cell proliferation assay, measured as a function of ^3H-thymidine incorporation, showed poor proliferation among the $CD4^+PD\text{-}1^+$ T cells after anti-CD3 mAb stimulation, whereas $CD4^+PD\text{-}1^-$ T cells proliferated normally in response to this stimulation (Fig. 2*G*). The proliferation capacity of the $CD4^+PD\text{-}1^+$ T cells on anti-CD3 mAb stimulation was partially restored by the addition of anti-CD28 mAb or recombinant human IL-2 (hIL-2). Thus, the $CD4^+PD\text{-}1^+$ T cells in NZB/W F1 mice had a low capacity for proliferation.

$CD4^+$ $CD25^-$ $PD\text{-}1^+$ T cells enforces anti–ds-DNA Ab production

To clarify if $CD4^+PD\text{-}1^+$ T cells help autoantibody production compared with $CD4^+$ $PD\text{-}1^-$ cells, both subsets from 16-wk-old NZB/W F1 mice were purified and stimulated with anti-CD3/CD28 mAbs, and cocultured with $B220^+$ splenocytes from 32-

wk-old NZB/W F1 mice. Because there was no difference between these subsets in IgG ds-DNA Ab production (data not shown), we then compared $CD4^+$ $CD25^-$ $PD\text{-}1^+$ and $CD4^+$ $CD25^-$ $PD\text{-}1^-$ T subsets. $CD4^+CD25^-$ $PD\text{-}1^+$ T cells tended to help produce more IgG ds-DNA Ab than $CD4^+CD25^-$ $PD\text{-}1^-$ T cells after stimulation with anti-CD3/CD28 mAbs ($p = 0.08$) (Fig. 2*F*).

Anti–PD-1 mAb treatment prevents glomerulonephritis

To test the effect of treating NZB/W F1 mice with anti–PD-1 mAb, we i.p. injected either anti–PD-1 mAb (J43) or control IgG (hamster IgG) into NZB/W F1 mice three times a week for 10 wk, beginning when they were 16–17 wk old. Surprisingly, 50% (5/10) of the anti–PD-1 mAb-treated mice were still alive at 44 wk of age, when all the control mice had died of severe nephritis ($p < 0.05$ by Fisher exact test, $p = 0.09$ by log-rank comparison test) (Fig. 3*A*), even though four of the five surviving mice had severe proteinurea. In addition, the anti–PD-1 mAb treatment tended to delay the onset of nephritis ($p = 0.07$, log-rank comparison test) (Fig. 3*A*). Notablely, serum IFN-γ level of anti–PD-1 mAb-treated mice (24 wk old, $n = 20$) was undetectable, whereas control mice (24 wk old, $n = 12$) were clearly separated into the high-serum IFN-γ group (>18 pg/ml, $n = 5$) and the low-serum IFN-γ group (<1 pg/ml, $n = 7$). Control mice with high-serum IFN-γ showed higher incidence of mortality (80% versus 14%) ($p < 0.05$, log-rank comparison test) and proteinuria ($p = 0.09$, log-rank comparison test) at 32 wk than those with low-serum IFN-γ (Fig. 3*A*).

PAS staining of the kidneys obtained from the control IgG-treated mice, which had died at 40 wk of age, revealed nephritis that was much more severe than in the anti–PD-1 mAb-treated mice sacrificed at 44 wk of age, which showed mesangial cell proliferation and capillary wall thickening (Fig. 3*B*). Surprisingly, immunofluorescence analysis showed markedly reduced staining of IgG2a, IgG, and C3 deposits in the glomeruli of the anti–PD-1 mAb-treated mice sacrificed at 40 wk of age, which was in contrast to the findings in the control mice and deceased anti–PD-1 mAb-treated mice (Fig. 3*C*).

For examining the numbers of $CD4^+PD\text{-}1^+$ T cells in the spleen after treatment, we used another clone of PD-1 Ab, RMP1-30, and the difference of epitopes was confirmed by the double staining of J43 and RMP1-30 with FACS (Supplemental Fig. 3). The percentage of $CD4^+PD\text{-}1^+$ T cells in the spleen was significantly lower in the anti–PD-1 mAb-treated mice at 24 wk old ($n = 3$), than in the control mice ($n = 3$) (mean ± SD; 4.6 ± 2.5% versus 14.2 ± 7.2%, $p < 0.05$) (Fig. 4*A*). The percentages of IFN-γ–producing $CD4^+PD\text{-}1^+$ T cells in the spleen were not statistically different between anti–PD-1 mAb-treated mice and control mice (Fig. 4*A*). To determine how the anti–PD-1 Ab reduced the number of $PD\text{-}1^+$ T cells in vivo, we examined the CDC of J43 Ab. J43, but not control hamster Ig significantly induced cell death to the $PD\text{-}1^+$ 11A1.6 mutant by CDC activity, as demonstrated by PI staining. Both PI staining and trypan blue exclusion methods showed comparable levels of cytotoxicity with J43 mAb (Supplemental Fig. 2).

Treatment with anti–PD-1 mAb decreases the $CD4^+PD\text{-}1^+$ T cells, IFN-γ production, and the production of IgG2a anti–ds-DNA Abs

We examined the effects of blocking PD-1 on the proportion of splenic $CD4^+PD\text{-}1^+$ T cells, IFN-γ production, and the production of IgG2a anti–ds-DNA Abs. The proportion of splenic $CD4^+PD\text{-}1^+$ T cells among $CD4^+$ T cells was significantly lower in the anti–PD-1 mAb-treated mice than in the control mice at 24 wk of age (Fig. 4*A*, *left panel*). The proportion of IFN-γ–producing $CD4^+$ $PD\text{-}1^+$ T cells among $CD4^+$ T cells was significantly lower in anti–PD-1 mAb-treated mice than control mice, although the proportion of IFN-γ–producing $CD4^+PD\text{-}1^+$ T cells among $CD4^+PD\text{-}1^+$ T cells showed no differences (Fig. 4*A*, *right panel*). The serum level of IFN-γ was significantly lower in the anti–PD-1 mAb-treated mice than control mice (24 wk old, Fig. 4*B*, *left panel*). In addition, the serum IgG2a ds-DNA Ab level was lower in anti–PD-1 mAb-treated mice than control mice (24 wk old, Fig. 4*B*, *right panel*).

Blocking PD-L1 with an anti–PD-L1 mAb increases mortality and accelerates nephritis

We next tested whether blocking PD-L1 with an anti–PD-L1 mAb would affect the development of nephritis in the NZB/W F1 mice. The anti–PD-L1 mAb-treated mice had an earlier onset of proteinuria and a higher mortality rate than the control mice (50% versus 10%, at 33 wk of age) (Fig. 5*A*), although the difference in mortality did not quite reach statistical significance ($p = 0.055$). On autopsy, all the mice that had died up to the age of 33 wk (five anti–PD-L1 mAb-treated mice and one rat–IgG-treated mouse) exhibited severe nephritis (unpublished observations). Notably, the anti–PD-L1 mAb-treated mice could be clearly separated into a high-serum IFN-γ group (>18 pg/ml, $n = 6$) and a low IFN-γ group (<1 pg/ml, $n = 4$). The mice with high-serum IFN-γ tended to have an earlier onset of proteinuria ($p = 0.12$, log-rank comparison test) and had a significantly higher mortality rate than those with low-serum IFN-γ (83% versus 25%, at 33 wk of age) ($p = 0.019$, log-rank comparison test) (Fig. 5*A*, *bottom*).

To explore the mechanism underlying the accelerated nephritis and increased mortality caused by the anti–PD-L1 mAb treatment, we performed histological analyses of kidneys harvested from anti–PD-L1 mAb-treated and control Ig-treated mice at 20 and 36 wk of age. PAS staining of kidney sections from 20-wk-old mice showed a significantly greater total number of glomerular cells in the kidneys of the anti–PD-L1 mAb-treated mice than in those of the control IgG-treated mice (Fig. 5*B*), showing that the anti–PD-L1 mAb-treated mice exhibited progressive mesangial hyperplasia. We next evaluated the kidneys of the 33-wk-old NZB/W F1 mice for glomerular sclerosis and tubular damages (atrophy or dilatation) using a scoring system (PAS staining), and found these changes to be more severe in the anti–PD-L1 mAb-treated than in the control IgG-treated mice ($p < 0.05$) (Fig. 5*C*). These histological findings confirmed that the anti–PD-L1 mAb treatment accelerated the development of glomerulonephritis and interstitial nephritis in the NZB/W F1 mice. On the other hand, mesangial hyperplasia in the glomeruli of 33-wk-old NZB/W F1 mice was more severe in the controls than in the anti–PD-L1 mAb-treated mice. This is the opposite of the situation in the 20-wk-old mice, and may be explained by the greater severity of the sclerosis in the anti–PD-L1 mAb-treated mice. The extent of the glomerular deposition of the IgG subclasses (IgG1, IgG2a, and IgG3) and C3 did not differ significantly between the two groups (S. Kasagi, S. Kawano, T. Okazaki, T. Honjo, A. Morinobu, S. Hatachi, K. Shimatani, Y. Tanaka, N. Minato, and S. Kumagai, unpublished observations).

Blockage of PD-L1 increases the $CD4^+PD\text{-}1^+$ T cells, and the production of IFN-γ, IL-10, and IgG2a anti–ds-DNA Abs

The proportion of splenic $CD4^+PD\text{-}1^+$ T cells was significantly higher in the anti–PD-L1 mAb-treated mice than in the control mice at 20–24 wk of age (Fig. 6*A*). In addition, serum levels of Th1 (IFN-γ, TNF-α) and Th2 (IL-4, IL-6, IL-10, TGF-β) cytokines in 20-wk-old mice were measured (Fig. 6*B*). The serum levels of both IFN-γ and IL-10 were significantly elevated in the anti–PD-L1 mAb-treated mice, but there were no significant

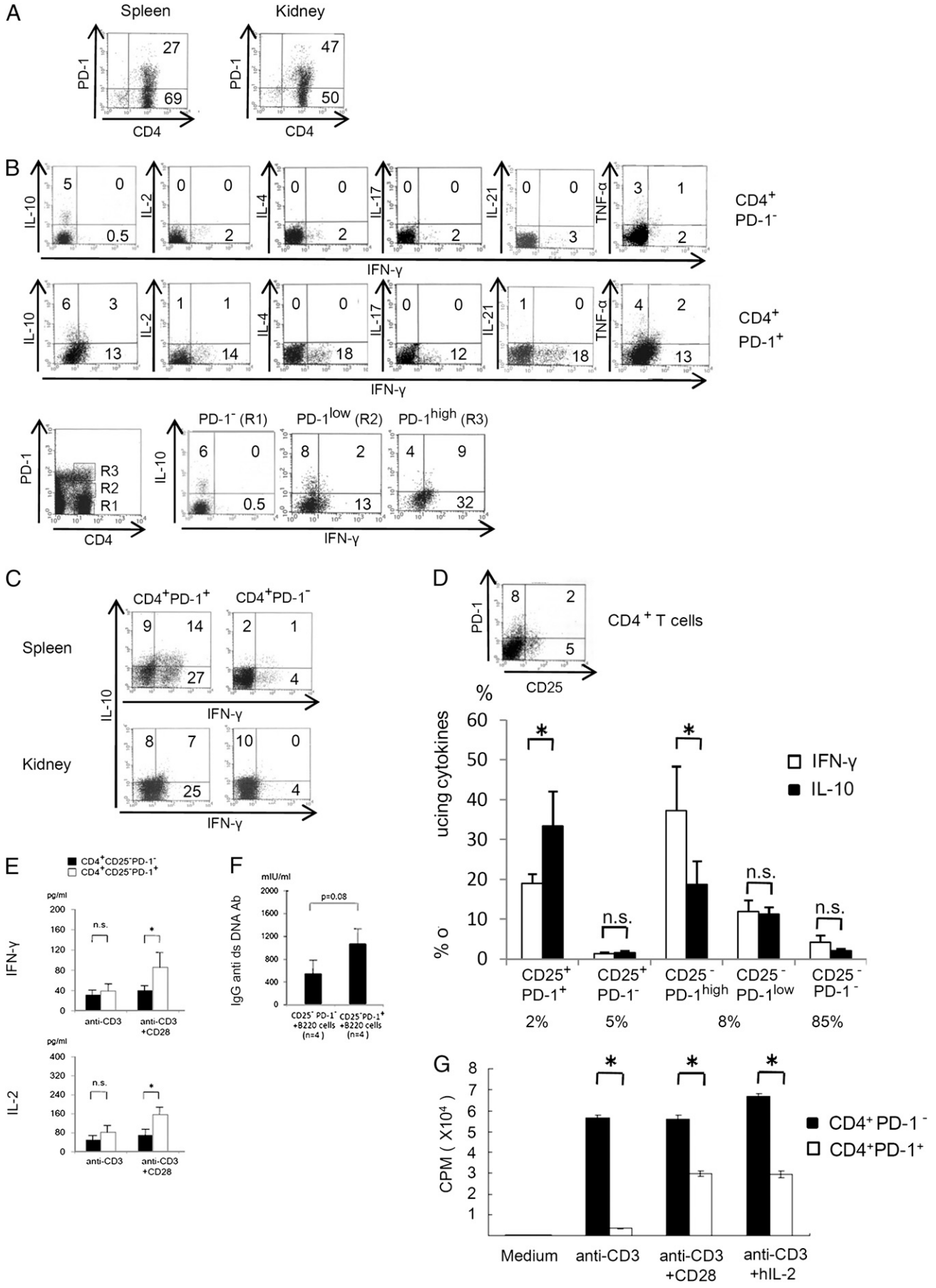

FIGURE 2. $CD4^+PD\text{-}1^{high}$ T cells produce a high level of IFN-γ but proliferate poorly upon stimulation in NZB/W F1 mice. *A*, Percentage of $CD4^+PD\text{-}1^+$ T cells in the spleen and kidney of nephritic mice at 36 wk of age. *B*, Intracellular cytokine expression in $CD4^+$ $PD\text{-}1^-$ T cells (*top panel*) and $CD4^+PD\text{-}1^+$

differences in the serum levels of TNF-α, IL-6, or TGF-β between the two groups. Serum IL-4 was not detectable in either the anti–PD-L1 mAb-treated or control mice. We also measured the serum titers of IgG subclasses and IgG2a anti–ds-DNA Ab, the most essential autoantibody in the pathogenesis of nephritis in NZB/W F1 mice, when the mice were 24 wk old. We found that the serum IgG2a, IgG3, and IgG2a anti–ds-DNA Ab levels were higher in 24-wk-old anti–PD-L1 mAb-treated mice whose serum IFN-γ was high (>18 pg/ml) at 20 wk of age than in 24-wk-old anti–PD-L1 mAb-treated mice whose serum IFN-γ was low (<1 pg/ml) at 20 wk of age, or in control mice (Fig. 7*A*, 7*B*). There were no differences in the serum levels of the IgG1 subclass among these three groups. These results suggest that the blockage of PD-L1 accelerated the onset of nephritis by enhancing the production of IFN-γ and IgG2a anti–ds-DNA Ab.

Table II. *Phenotypic characteristics of splenic CD4$^+$PD-1$^+$ T cells (NZB/W F1, 16 wk old)*

Molecule	CD4$^+$PD-1^{+a}	CD4$^+$PD-1^{-a}	*P*
CD25	15.1 ± 7.5	6.0 ± 1.7	< 0.005
CD28	98.5 ± 1.5	97.4 ± 2.5	–
CD44^{high}	81.9 ± 1.4	54.6 ± 2.0	< 0.05
CD62L^{high}	31.9 ± 1.5	67.3 ± 6.9	< 0.05
CD69	26.2 ± 1.7	1.7 ± 0.9	< 0.05
CD80	29.2 ± 1.9	2.3 ± 0.9	< 0.05
CD86	35.6 ± 15.5	1.9 ± 0.2	< 0.05
CTLA-4	36.9 ± 14.5	0.5 ± 0.4	< 0.05
BTLA	48.7 ± 10.2	2.4 ± 2.6	< 0.05
TCRβ	96.8 ± 0.2	98.8 ± 0.3	–
TCRγδ	4.0 ± 1.6	1.3 ± 0.2	< 0.05
CD25$^+$FoxP3$^+$	4.4 ± 1.6	0.3 ± 0.2	< 0.005

CD4$^+$ splenocytes were harvested from 16-wk-old NZB/W F1 mice (n = 3) with MACS, and cell surface Ags or intracellular Foxp3 expression was analyzed with four color FACS analysis.

[a] n = 3.

Discussion

SLE is an autoimmune disease characterized by multiple immune system defects, including CD4$^+$ T and B cell hyper-reactivity and abnormal cytokine and autoantibody production. However, despite its being implicated in SLE, whether the immunoregulatory function of the PD-1/PD-L pathway functions properly in SLE has been unclear. With this question in mind, we used NZB/W F1 mice as a model to investigate the contribution of the PD-1/PD-L1 pathway to SLE. Notably, in vivo treatment with an anti–PD-1 mAb significantly reduced the mortality rate of NZB/W F1 female mice. Furthermore, anti–PD-1 mAb treatment dramatically reduced the renal infiltration by lymphocytes and splenic infiltration by CD4$^+$PD-1$^+$ T cells and delayed the development of nephritis. Given that the mortality of unmanipulated NZB/W F1 female mice in our colony was 95% at 48 wk of age (S. Kasagi et al., unpublished observations), it was surprising that 50% of the anti–PD-1 mAb-treated mice remained alive at age 11 mo. We found decreased numbers of PD-1$^+$ T cells in vivo, and confirmed that the anti–PD-1 mAb, J43, triggered CDC in PD-1$^+$ T cells in vitro. In addition, we detected that the percentages of IFN-γ–producing CD4$^+$ PD-1$^+$ T cells was not statistically different between anti–PD-1 mAb-treated mice and control mice in vitro, which implied that J43 did not downregulate the intracellular machinery of IFN-γ production in CD4$^+$PD-1$^+$ T cells. Therefore, the in vivo effect of J43 mAb can be explained by the depletion of PD-1$^+$ T cells, as evidenced by the histological absence of PD-1–positive cells in kidney sections from survived anti–PD-1–treated mice, although we could not absolutely rule out another possible mechanism of action (i.e., the downregulation of PD-1 expression on lymphocytes). J43 Ab has been considered to be a neutralizing Ab, and injection of J43 exacerbated experimental allergic encephalitis (EAE) and NOD diabetes (25, 26). Those reports seem to be opposite to our result. One explanation is the peculiarity of NZB/W F1 mice. NZB/W F1 mice show the property of an immune-complex–mediated disease, whereas both NOD and EAE mice are not regarded as immune-complex–mediated diseases. Another explanation is that the activation stage of CD4$^+$PD-1$^+$ T cells targeted by anti–PD-1 mAb, J43, may be different between NZB/W F1 and NOD/EAE mice. The nephritis of NZB/W F1 mice develops more chronically than the diabetes of NOD or the encephalitis of EAE mice. The effector/memory CD4$^+$PD-1$^+$ T cells in spleens or kidneys of NZB/W F1 mice are relatively resistant to inhibitory signals mediated by PD1–PD-L1 interactions, because CD4$^+$PD-1$^+$ T cells survive and accumulate in inflamed tissue where PD-L1 is highly expressed. On the other hand, CD4$^+$PD-1$^+$ T cells in NOD/EAE mice may be newly arising and susceptible to inhibition by PD1–PD-L1 interactions. Therefore, it is plausible that the CDC activity of J43 is dominantly exerted in NZB/W F1 mice, whereas the blocking activity of J43 is dominant in NOD and EAE mice. These diverse effects by anti–PD-1 Ab are of great interest and further investigations are anticipated.

In contrast, anti–PD-L1 mAb treatment in vivo accelerated nephritis. This discrepancy might be owing to the anti–PD-L1 mAb, 111A, functioning as a blocking Ab of the PD-1/PD-L1 interaction. In accordance with this idea, the proportion of PD-1$^+$ cells among splenic CD4$^+$ T cells was significantly increased after anti–PD-L1 mAb treatment. The next question is whether the increase in CD4$^+$PD-1$^+$ cells is the cause or the result of disease progression. It is generally accepted that the autoantigen-specific CD4$^+$ T cells, which produce large quantities of IFN-γ, cause severe nephritis in NZB/W F1 mice (2, 27). In this study, we demonstrated that the CD4$^+$PD-1^{high} T cells are high IFN-γ producers and of the typical effector/memory phenotype, CD62L^{low} CD69^{high}CD44^{high}. Furthermore, we showed that CD4$^+$CD25$^-$ PD-1$^+$ T cells produced larger amount of IFN-γ than CD4$^+$CD25$^-$ PD-1$^-$ T cells, and helped B cells produce IgG ds-DNA Ab. Hence, we propose that the CD4$^+$PD-1^{high} T cell is not a bystander cell recruited to local inflammation, but a strong candidate for the pathogenic T cell that causes nephritis in NZB/W F1 mice.

PD-1 is regarded as a receptor that is crucial for maintaining peripheral tolerance. The notable characteristics of the CD4$^+$PD-1^{high} T cells in this study were low IL-2 production, poor proliferative capacity, and high IFN-γ production. The low IL-2 production and poor proliferative capacity are seemingly compatible with the characteristics of anergic T cells, which are

T cells (*middle panel*) in prenephritic mice at 16 wk of age. R1, R2, and R3 represent CD4$^+$PD-1$^-$, CD4$^+$PD-1^{low}, and CD4$^+$PD-1^{high} T cells, respectively (*bottom panel*). *C*, Dual staining of intracellular IFN-γ/IL-10 of CD4$^+$PD-1$^+$ T cells in the kidney and spleen from nephritic mice at 36 wk of age. *D*, Percentage of intracellular IFN-γ/IL-10–producing CD4$^+$ T cells (16-wk-old spleen). CD4$^+$ T cells were separately analyzed for CD25 and PD-1. *E*, CD4$^+$ CD25$^-$ PD-1$^+$ and CD4$^+$ CD25$^-$ PD-1$^-$ T cells (16-wk-old spleen) were stimulated with anti-CD3 and anti-CD3/CD28, and supernatant were measured for IFN-γ and IL-2 with ELISA. *F*, B220$^+$ cells were cocultured with CD4$^+$ CD25$^-$ PD-1$^+$ or CD4$^+$ CD25$^-$ PD-1$^-$ T cells in the presence of anti-CD3/CD28 stimulation, and production of IgG ds-DNA Ab in the supernatant was measured with ELISA. *G*, Uptake of ^{3}H-thymidine by splenic CD4$^+$ PD-1$^+$ (open bars) and CD4$^+$ PD-1$^-$ (closed bars) T cells after stimulation with anti-CD3 alone, or with anti-CD28 or hIL-2 (16 wk old).

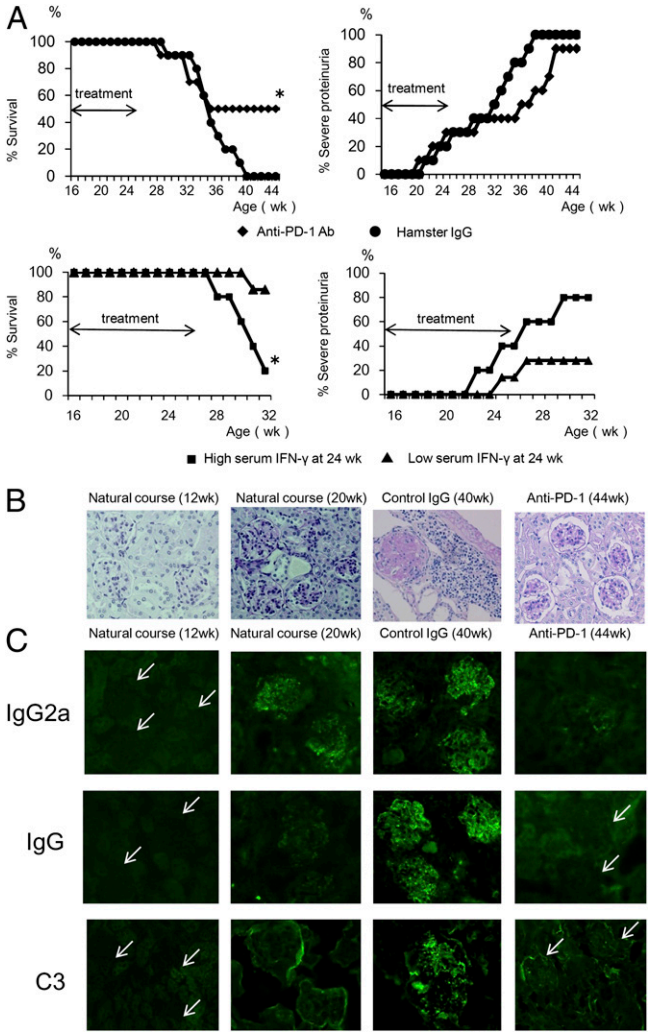

FIGURE 3. Anti–PD-1 mAb treatment delays the onset of nephritis and prolongs survival. *A*, Kaplan-Mayer survival graphs of anti–PD-1 mAb-treated (◆; $n = 10$) and control IgG-treated (●; $n = 10$) mice are shown. The anti–PD-1 mAb-treated group showed a lower mortality than the control group ($*p < 0.05$; Fisher exact test; *left upper panel*). Graph shows the percentage of mice developing severe nephritis (>300 mg/dl), as defined in *Materials and Methods*. Anti–PD-1 mAb treatment tended to delay the onset of severe nephritis ($p = 0.07$, log-rank comparison test; *right upper panel*). When control mice (24 wk old; $n = 12$) were separated into a high-serum IFN-γ group (>18 pg/ml; ■; $n = 5$) and a low-serum IFN-γ group (<1 pg/ml; ▲; $n = 7$), the former showed higher incidence of mortality ($*p < 0.05$, log-rank comparison test; *left lower panel*) and proteinuria ($p = 0.09$, log-rank comparison test) than the latter (*right lower panel*). *B*, PAS staining of the kidneys from control IgG-treated and anti–PD-1 mAb-treated mice. Representative pictures are shown. *C*, Immunofluorescent staining for IgG2a, IgG, and C3 deposits in the glomeruli of prenephritic (12 and 20 wk old), control IgG-treated (40 wk old), and anti–PD-1 mAb-treated (44 wk old) mice. Arrows indicate glomeruli. Representative pictures are shown. Original magnification ×100 (*B*) and ×200 (*C*).

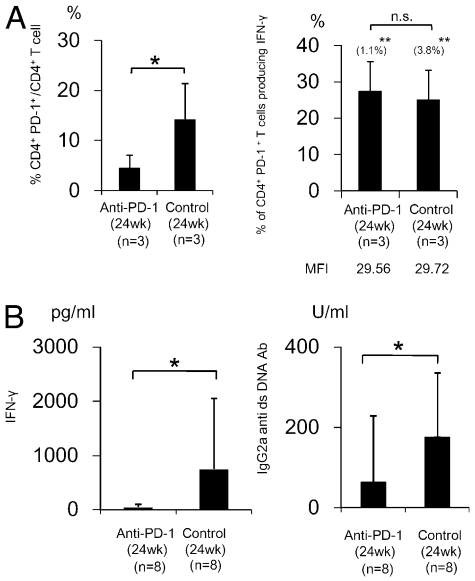

FIGURE 4. Anti–PD-1 mAb treatment decreased the PD-1$^+$ cells. *A*, The percentages of PD-1$^+$ T cells among CD4$^+$ T cells of 24-wk-old euthanized anti–PD-1 mAb-treated mice and control mice are shown (*left panel*). The percentages of IFN-γ–producing CD4$^+$PD-1$^+$ T cells among CD4$^+$ PD-1$^+$ T cells (*right panel*), and those of IFN-γ–producing CD4$^+$PD-1$^+$ T cells among CD4$^+$ T cells are also shown (**). Mean fluorescence intensities of IFN-γ–producing CD4$^+$PD-1$^+$ T cells among CD4$^+$PD-1$^+$ T cells in anti–PD-1 mAb-treated mice and control mice are shown at the bottom. *B*, Serum levels of IFN-γ, IgG2 ds-DNA Ab at 24 wk of age are shown.

thought to have a role in maintaining peripheral tolerance. However, T cells from old NZB/W F1 mice (8–9 mo old) are reported to generally have low IL-2 productivity (28), with the effector T cells showing a poorer proliferative response than naive T cells on antigenic stimulation in vitro (29). In addition, the expression pattern of cell-surface Ags on the CD4$^+$PD-1^{high} T cells and high IFN-γ production are not typical of anergic T cells. Therefore, we conclude that the CD4$^+$PD-1^{high} T cells are not anergic T cells, and their increase in the kidney is not the simple accumulation of anergic T cells. In human autoimmune diseases, a similar type of CD4$^+$PD-1$^+$ T cell that produces IFN-γ has been shown to accumulate at inflammatory sites (17–19). Thus, it will be intriguing to elucidate the detailed mechanism underlying the accumulation of CD4$^+$PD-1^{high} T cells, which is still largely unknown.

The IFN-γ produced by CD4$^+$ T cells is responsible for IgG class switch, IgG2a anti–ds-DNA Ab production, and mesangial cell hyperplasia in NZB/W F1 mice (27, 30–32). Anti–PD-1 mAb treatment dramatically reduced serum levels of IFN-γ at 24 wk of age. On the contrary, five of six mice that had high-serum levels of IFN-γ at 20 wk of age showed high-serum levels of anti-IgG2a ds-DNA Ab after receiving anti–PD-L1 mAb injections and died of nephritis, suggesting that the PD-L1 signal might suppress the production of IFN-γ and consequently of the IgG2a anti–ds-DNA Ab in NZB/W F1 mice. Recently, several studies showed that the tissue-specific expression of PD-L1 is functionally important and plays a key role in protecting against pathogenic self-reactive T cells (26, 33). Other recent reports have shown that IFN-γ induces the expression of PD-L1 on murine renal tubular epithelial cells and human endothelial cells, and that the IFN-γ synthesis by T cells is suppressed by PD-L1 in vitro (34, 35). Nevertheless, several reports showed that upregulated expression of PD-L1 in inflamed tissue failed to suppress disease (16, 26). Taken together, these findings indicate that the role of PD-L1 in protecting renal tissue from CD4$^+$PD-1$^+$ T cells is insufficient at the nephritic stage in NZB/W F1 mice.

The finding that CD4$^+$PD-1^{high} T cells are high IFN-γ producers is interesting when we consider the features of CD8$^+$ PD-1^{high} T cells in chronic viral infections. The CD8$^+$PD-1^{high} T cells in chronic lymphocytic choriomeningitis virus or HIV infections have been defined recently as "exhausted T cells" (36, 37). These CD8$^+$ PD-1^{high} T cells are reportedly dysfunctional with respect to cytokine secretion (IFN-γ, TNF-α, IL-2) and proliferation, and are

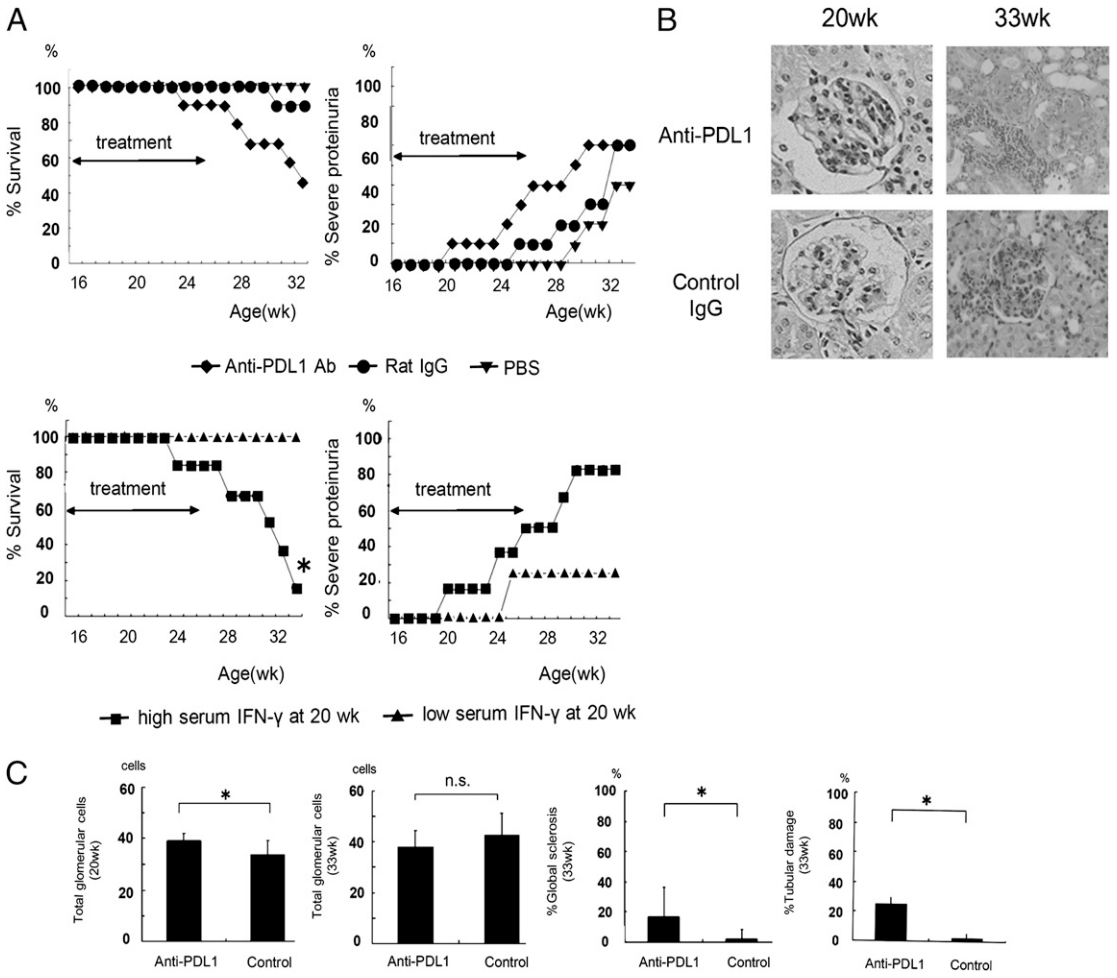

FIGURE 5. Blockage of PD-L1 accelerates the nephritis of NZB/W F1 mice. *A*, Kaplan-Mayer survival graphs for mice treated with the anti–PD-L1 mAb (♦; $n = 10$), control IgG (●; $n = 10$), or PBS ($n = 10$, ▼) were shown (*left upper panel*). The percentage of mice with severe proteinuria (>300 mg/dl) are shown (*right upper panel*). Anti–PD-L1 mAb-treated mice are separated into two groups, those with high-serum IFN-γ (>18 pg/ml) at 20 wk of age ($n = 6$, ■); and those with low-serum IFN-γ (<1 pg/ml) at 20 wk of age ($n = 4$, ▲). (*Lower left panel*) Kaplan-Mayer survival graphs for the groups with high- and low-serum IFN-γ are shown. The percentage of mice with severe proteinuria (>300 mg/dl) in the groups with high- and low-serum IFN-γ are shown (*lower right panel*). *B*, Representative histological features of the kidneys from anti–PD-L1 mAb-treated and control IgG-treated mice at 20 and 33 wk of age are shown. All sections were stained with PAS (original magnification ×400). *C*, Mesangial cell hyperplasia, interstitial lymphocytic infiltration, and tubular damage were evaluated as described in *Materials and Methods*, and the values at 20 and 33 wk of age are plotted. $*p < 0.05$.

unable to eliminate infected cells in the absence of the anti–PD-L1 Ab. Anti–PD-L1 mAb treatment restores the function of the exhausted $CD8^+PD\text{-}1^{high}$ T cells, indicating that they remain capable of mediating inhibitory signaling via the PD-1 receptor. The attenuated cellular proliferation and low IL-2 production of the $CD4^+PD\text{-}1^{high}$ T cells are similar to those of $CD8^+$ $PD\text{-}1^{high}$ T cells. However, the $CD4^+PD\text{-}1^{high}$ T cells are not exhausted, in terms of their high IFN-γ production. It will be intriguing to evaluate the capabilities of $CD4^+PD\text{-}1^{high}$ T cells in chronic autoimmune diseases in comparison with those of $CD8^+PD\text{-}1^{high}$ T cells in chronic viral infections. The $CD4^+PD\text{-}1^+$ T cells also included an IL-10–producing fraction, which showed a $CD4^+$ $CD25^+$ or $CD4^+CD25^-CD45RB^{low}$ phenotype, as a minor population. These two T cell phenotypes resembled those of Treg cells or Tr1 cells. Ding et al. reported that PD-L1–Ig induces Tr1 differentiation from naive $CD4^+$ T cells in an IFN-γ–dependent manner, and Tr1 downregulates Th1 immunity in vitro (38). Our findings thus support the possibility that IL-10–producing $CD4^+$ $PD\text{-}1^+$ T cells functioning as Treg or Tr1 cells might counteract the IFN-γ–producing $CD4^+PD\text{-}1^{high}$ T cells in NZB/W F1 mice. In contrast, several reports indicate that IL-10 secreted from B cells augments autoantibody production and accelerates the development of nephritis (39–42). Thus, it is still uncertain if the IL-10 produced by $CD4^+$ T cells has a pathogenic or a regulatory role during the development of nephritis in NZB/W F1 mice, and further investigation will be needed to clarify this issue.

In our study, immunoregulatory molecules (e.g., BTLA, CTLA-4, and CD80) were concomitantly expressed on $CD4^+PD\text{-}1^{high}$ T cells in NZB/W F1 mice. Both BTLA and CTLA-4 are usually expressed on activated T cells and, like PD-1, inhibit IFN-γ production (6, 44, 45), indicating that the inhibitory signaling by BTLA and CTLA-4 on $CD4^+PD\text{-}1^{high}$ T cells is not sufficient to suppress IFN-γ production. CD80 (B7.1) is one of two ligands (CD80 and CD86) that bind CTLA-4 and CD28, and is induced on both activated T cells and APCs. In addition, one recent report showed that CD80 on T cells may act as a regulatory receptor for PD-L1 expressed on APCs (46), whereas another showed that blockade of CD80 by an anti-CD80 mob inhibits IgG2a ds-DNA Ab production in vivo, and that the administration of both anti-CD80 and anti-CD86 mAbs prevents autoantibody production and

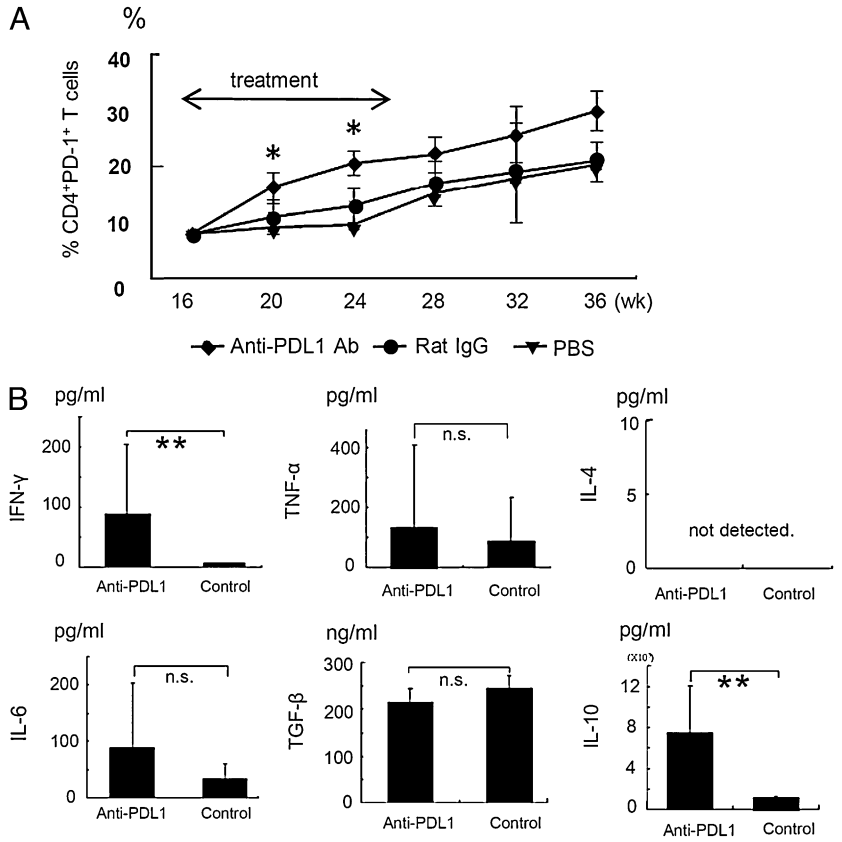

FIGURE 6. Blockage of PD-L1 accelerates the production of IFN-γ and IL-10. *A*, Percentage of PD-1$^+$ cells among splenic CD4$^+$ T cells. The percentage of CD4$^+$PD-1$^+$ T cells was significantly increased in the anti–PD-L1 mAb-treated mice (♦; $n = 10$), compared with the control IgG-treated (●; $n = 10$) and PBS-treated mice (▼; $n = 10$) ($* p < 0.05$). *B*, Effects of anti–PD-L1 mAb treatment on the serum levels of cytokines in 20-wk-old mice ($** p < 0.01$). Anti–PD-L1 mAb treatment augmented the production of IFN-γ and IL-10.

nephritis in NZB/W F1 mice (47). The implication of these findings is that the CD80 on T cells mainly mediates stimulatory rather than negative regulatory signals in NZB/W F1 mice. Therefore, the anti–PD-L1 mAb treatment might also block the CD80-mediated regulatory signaling to CD4$^+$PD1$^+$CD80$^+$ T cells, but its contribution is uncertain. That said, based on the findings summarized previously, we hypothesize that CD4$^+$PD-1^{high} T cells evade negative regulation by inhibitory receptors such as CD80, CTLA-4, and BTLA, as well as PD-1.

We observed that the CD4$^+$PD-1$^+$ T cells increased with age in both NZB and NZB/W F1 mice, and that the B220$^+$PD-1$^+$ cells increased with age in NZB mice, whereas neither of these cell types increased in the NZW or BALB/c mice. Both NZB and NZB/W F1 mice naturally develop lupus-like nephritis, whereas male NZW mice and BALB/c mice are clinically healthy. The clinical manifestations of lupus-like nephritis in NZB mice differ from those in NZB/W F1 mice in that the NZB mice develop severe autoimmune hemolytic anemia and mild glomerulonephritis (48). As is the case with NZB F1 mice, in NZB mice, the IFN-γ–producing Th1 cells mediate the production of antierythrocyte Abs and accelerate the progression of autoimmune hemolytic anemia (49). In addition, we found that the pattern of expression of intracellular cytokines and cell-surface Ags in the splenic CD4$^+$PD-1$^+$ T cells from NZB mice was very similar to that of CD4$^+$PD-1$^+$ T cells from NZB/W F1 mice (unpublished observations). This suggests that the CD4$^+$PD-1$^+$ T cells are a good marker for the autoimmune phenomena of both mouse strains, and that the common genetic background of these mice contributes to the increased number of CD4$^+$PD-1$^+$ T cells, which may be key players in the broken tolerance seen in these mice.

In summary, we showed that IFN-γ–producing CD4$^+$PD-1^{high} T cells play a key role in the progression of murine lupus nephritis. It would be intriguing to examine their functions in other autoimmune diseases, even though it is still necessary to dissect the molecular mechanisms underlying the dysregulation of PD-1 signaling in CD4$^+$PD-1^{high} T cells. Finally, we propose that the elimination of CD4$^+$PD-1$^+$ T cells using an anti–PD-1 mAb might represent a novel therapeutic strategy for the treatment of human lupus nephritis.

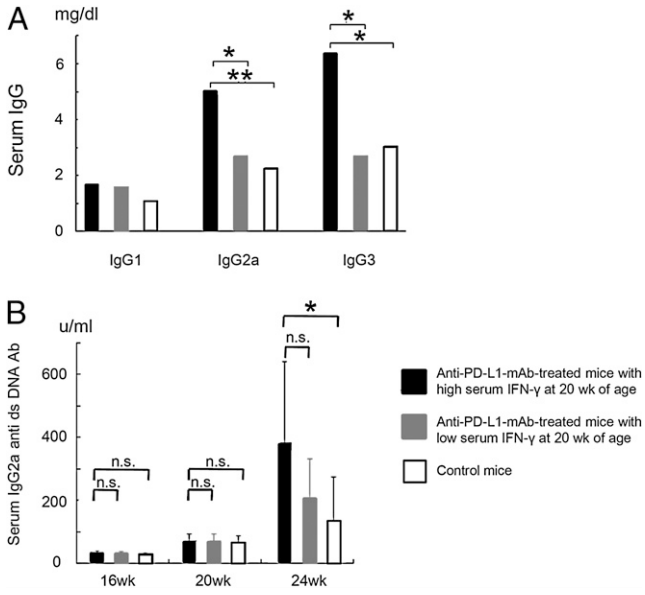

FIGURE 7. Blockage of PD-L1 induces IgG class switch and IgG2a ds-DNA Ab production in NZB/W F1 mice. Effects of anti–PD-L1 mAb treatment on serum levels of (*A*) IgG subclasses in 24-wk-old mice, and (*B*) IgG2a anti–ds-DNA Ab in mice at 16, 20, or 24 wk of age are shown. *A, B*, black bar, anti–PD-L1 mAb-treated mice with high-serum IFN-γ (>18 pg/ml) at 20 wk of age; gray bar, anti–PD-L1 mAb-treated mice with low-serum IFN-γ (<1 pg/ml) at 20 wk of age; white bar, control mice. $* p < 0.05$; $** p < 0.01$.

Acknowledgments

We are grateful to Dr. Daikuke Sugiyama for statistical analysis and Dr. Hirokazu Kurata and Y. Miyamoto for excellent technical assistance. We are also grateful to Dr. Grace Gray for English editing.

Disclosures

The authors have no financial conflicts of interest.

References

1. Datta, S. K., A. Kaliyaperumal, and A. Desai-Mehta. 1997. T cells of lupus and molecular targets for immunotherapy. *J. Clin. Immunol.* 17: 11–20.
2. Andrews, B. S., R. A. Eisenberg, A. N. Theofilopoulos, S. Izui, C. B. Wilson, P. J. McConahey, E. D. Murphy, J. B. Roths, and F. J. Dixon. 1978. Spontaneous murine lupus-like syndromes. Clinical and immunopathological manifestations in several strains. *J. Exp. Med.* 148: 1198–1215.
3. Lin, L. C., Y. C. Chen, C. C. Chou, K. H. Hsieh, and B. L. Chiang. 1995. Dysregulation of T helper cell cytokines in autoimmune prone NZB x NZW F1 mice. *Scand. J. Immunol.* 42: 466–472.
4. Laskin, C. A., J. D. Taurog, P. A. Smathers, and A. D. Steinberg. 1981. Studies of defective tolerance in murine lupus. *J. Immunol.* 127: 1743–1747.
5. Mudd, P. A., B. N. Teague, and A. D. Farris. 2006. Regulatory T cells and systemic lupus erythematosus. *Scand. J. Immunol.* 64: 211–218.
6. Parry, R. V., J. M. Chemnitz, K. A. Frauwirth, A. R. Lanfranco, I. Braunstein, S. V. Kobayashi, P. S. Linsley, C. B. Thompson, and J. L. Riley. 2005. CTLA-4 and PD-1 receptors inhibit T-cell activation by distinct mechanisms. *Mol. Cell. Biol.* 25: 9543–9553.
7. Sharpe, A. H., E. J. Wherry, R. Ahmed, and G. J. Freeman. 2007. The function of programmed cell death 1 and its ligands in regulating autoimmunity and infection. *Nat. Immunol.* 8: 239–245.
8. Ishida, Y., Y. Agata, K. Shibahara, and T. Honjo. 1992. Induced expression of PD-1, a novel member of the immunoglobulin gene superfamily, upon programmed cell death. *EMBO J.* 11: 3887–3895.
9. Nishimura, H., N. Minato, T. Nakano, and T. Honjo. 1998. Immunological studies on PD-1 deficient mice: implication of PD-1 as a negative regulator for B cell responses. *Int. Immunol.* 10: 1563–1572.
10. Liang, S. C., Y. E. Latchman, J. E. Buhlmann, M. F. Tomczak, B. H. Horwitz, G. J. Freeman, and A. H. Sharpe. 2003. Regulation of PD-1, PD-L1, and PD-L2 expression during normal and autoimmune responses. *Eur. J. Immunol.* 33: 2706–2716.
11. Okazaki, T., Y. Iwai, and T. Honjo. 2002. New regulatory co-receptors: inducible co-stimulator and PD-1. *Curr. Opin. Immunol.* 14: 779–782.
12. Nishimura, H., M. Nose, H. Hiai, N. Minato, and T. Honjo. 1999. Development of lupus-like autoimmune diseases by disruption of the PD-1 gene encoding an ITIM motif-carrying immunoreceptor. *Immunity* 11: 141–151.
13. Nishimura, H., T. Okazaki, Y. Tanaka, K. Nakatani, M. Hara, A. Matsumori, S. Sasayama, A. Mizoguchi, H. Hiai, N. Minato, and T. Honjo. 2001. Autoimmune dilated cardiomyopathy in PD-1 receptor-deficient mice. *Science* 291: 319–322.
14. Okazaki, T., and T. Honjo. 2005. Pathogenic roles of cardiac autoantibodies in dilated cardiomyopathy. *Trends Mol. Med.* 11: 322–326.
15. Ferreiros-Vidal, I., J. J. Gomez-Reino, F. Barros, A. Carracedo, P. Carreira, F. Gonzalez-Escribano, M. Liz, J. Martin, J. Ordi, J. L. Vicario, and A. Gonzalez. 2004. Association of PDCD1 with susceptibility to systemic lupus erythematosus: evidence of population-specific effects. *Arthritis Rheum.* 50: 2590–2597.
16. Bertsias, G. K., M. Nakou, C. Choulaki, A. Raptopoulou, E. Papadimitraki, G. Goulielmos, H. Kritikos, P. Sidiropoulos, M. Tzardi, D. Kardassis, et al. 2009. Genetic, immunologic, and immunohistochemical analysis of the programmed death 1/programmed death ligand 1 pathway in human systemic lupus erythematosus. *Arthritis Rheum.* 60: 207–218.
17. Hatachi, S., Y. Iwai, S. Kawano, S. Morinobu, M. Kobayashi, M. Koshiba, R. Saura, M. Kurosaka, T. Honjo, and S. Kumagai. 2003. CD4+ PD-1+ T cells accumulate as unique anergic cells in rheumatoid arthritis synovial fluid. *J. Rheumatol.* 30: 1410–1419.
18. Bolstad, A. I., H. G. Eiken, B. Rosenlund, M. E. Alarcón-Riquelme, and R. Jonsson. 2003. Increased salivary gland tissue expression of Fas, Fas ligand, cytotoxic T lymphocyte-associated antigen 4, and programmed cell death 1 in primary Sjögren's syndrome. *Arthritis Rheum.* 48: 174–185.
19. Kobayashi, M., S. Kawano, S. Hatachi, C. Kurimoto, T. Okazaki, Y. Iwai, T. Honjo, Y. Tanaka, N. Minato, T. Komori, et al. 2005. Enhanced expression of programmed death-1 (PD-1)/PD-L1 in salivary glands of patients with Sjögren's syndrome. *J. Rheumatol.* 32: 2156–2163.
20. Oikawa, T., H. Takahashi, T. Ishikawa, A. Hokari, N. Otsuki, M. Azuma, M. Zeniya, and H. Tajiri. 2007. Intrahepatic expression of the co-stimulatory molecules programmed death-1, and its ligands in autoimmune liver disease. *Pathol. Int.* 57: 485–492.
21. Agata, Y., A. Kawasaki, H. Nishimura, Y. Ishida, T. Tsubata, H. Yagita, and T. Honjo. 1996. Expression of the PD-1 antigen on the surface of stimulated mouse T and B lymphocytes. *Int. Immunol.* 8: 765–772.
22. Ishida, M., Y. Iwai, Y. Tanaka, T. Okazaki, G. J. Freeman, N. Minato, and T. Honjo. 2002. Differential expression of PD-L1 and PD-L2, ligands for an inhibitory receptor PD-1, in the cells of lymphohematopoietic tissues. *Immunol. Lett.* 84: 57–62.
23. Heijnen, I. A., M. J. Glennie, and J. G. van de Winkel. 1997. Lysis of murine B lymphoma cells by transgenic phagocytes via a human FcγRI x murine MHC class II bispecific antibody. *Cancer Immunol. Immunother.* 45: 166–170.
24. Nozaki, Y., T. Yamagata, B. S. Yoo, M. Sugiyama, S. Ikoma, K. Kinoshita, M. Funauchi, and A. Kanamaru. 2005. The beneficial effects of treatment with all-trans-retinoic acid plus corticosteroid on autoimmune nephritis in NZB/WF mice. *Clin. Exp. Immunol.* 139: 74–83.
25. Salama, A. D., T. Chitnis, J. Imitola, M. J. Ansari, H. Akiba, F. Tushima, M. Azuma, H. Yagita, M. H. Sayegh, and S. J. Khoury. 2003. Critical role of the programmed death-1 (PD-1) pathway in regulation of experimental autoimmune encephalomyelitis. *J. Exp. Med.* 198: 71–78.
26. Ansari, M. J., A. D. Salama, T. Chitnis, R. N. Smith, H. Yagita, H. Akiba, T. Yamazaki, M. Azuma, H. Iwai, S. J. Khoury, et al. 2003. The programmed death-1 (PD-1) pathway regulates autoimmune diabetes in nonobese diabetic (NOD) mice. *J. Exp. Med.* 198: 63–69.
27. Jacob, C. O., P. H. van der Meide, and H. O. McDevitt. 1987. In vivo treatment of (NZB X NZW)F1 lupus-like nephritis with monoclonal antibody to gamma interferon. *J. Exp. Med.* 166: 798–803.
28. Sato, M. N., P. Minoprio, S. Avrameas, and T. Ternynck. 1995. Defects in the regulation of anti-DNA antibody production in aged lupus-prone (NZB x NZW) F1 mice: analysis of T-cell lymphokine synthesis. *Immunology* 85: 26–32.
29. Gajewski, T. F., S. R. Schell, G. Nau, and F. W. Fitch. 1989. Regulation of T-cell activation: differences among T-cell subsets. *Immunol. Rev.* 111: 79–110.
30. La Cava, A., F. M. Ebling, and B. H. Hahn. 2004. Ig-reactive CD4+CD25+ T cells from tolerized (New Zealand Black x New Zealand White)F1 mice suppress in vitro production of antibodies to DNA. *J. Immunol.* 173: 3542–3548.
31. Enghard, P., D. Langnickel, and G. Riemekasten. 2006. T cell cytokine imbalance towards production of IFN-γ and IL-10 in NZB/W F1 lupus-prone mice is associated with autoantibody levels and nephritis. *Scand. J. Rheumatol.* 35: 209–216.
32. Schwarz, M., M. Wahl, K. Resch, and H. H. Radeke. 2002. IFNγ induces functional chemokine receptor expression in human mesangial cells. *Clin. Exp. Immunol.* 128: 285–294.
33. Keir, M. E., S. C. Liang, I. Guleria, Y. E. Latchman, A. Qipo, L. A. Albacker, M. Koulmanda, G. J. Freeman, M. H. Sayegh, and A. H. Sharpe. 2006. Tissue expression of PD-L1 mediates peripheral T cell tolerance. *J. Exp. Med.* 203: 883–895.
34. Schoop, R., P. Wahl, M. Le Hir, U. Heemann, M. Wang, and R. P. Wüthrich. 2004. Suppressed T-cell activation by IFN-γ-induced expression of PD-L1 on renal tubular epithelial cells. *Nephrol. Dial. Transplant.* 19: 2713–2720.
35. Mazanet, M. M., and C. C. Hughes. 2002. B7-H1 is expressed by human endothelial cells and suppresses T cell cytokine synthesis. *J. Immunol.* 169: 3581–3588.
36. Barber, D. L., E. J. Wherry, D. Masopust, B. Zhu, J. P. Allison, A. H. Sharpe, G. J. Freeman, and R. Ahmed. 2006. Restoring function in exhausted CD8 T cells during chronic viral infection. *Nature* 439: 682–687.
37. Day, C. L., D. E. Kaufmann, P. Kiepiela, J. A. Brown, E. S. Moodley, S. Reddy, E. W. Mackey, J. D. Miller, A. J. Leslie, C. DePierres, et al. 2006. PD-1 expression on HIV-specific T cells is associated with T-cell exhaustion and disease progression. *Nature* 443: 350–354.
38. Ding, Q., L. Lu, B. Wang, Y. Zhou, Y. Jiang, X. Zhou, L. Xin, Z. Jiao, and K. Y. Chou. 2006. B7H1-Ig fusion protein activates the $CD4^+$ IFN-γ receptor$^+$ type 1 T regulatory subset through IFN-γ-secreting Th1 cells. *J. Immunol.* 177: 3606–3614.
39. Ye, Y. L., J. L. Suen, Y. Y. Chen, and B. L. Chiang. 1998. Phenotypic and functional analysis of activated B cells of autoimmune NZB x NZW F1 mice. *Scand. J. Immunol.* 47: 122–126.
40. Hahn, B. H., F. Ebling, R. R. Singh, R. P. Singh, G. Karpouzas, and A. La Cava. 2005. Cellular and molecular mechanisms of regulation of autoantibody production in lupus. *Ann. N. Y. Acad. Sci.* 1051: 433–441.
41. Ishida, H., T. Muchamuel, S. Sakaguchi, S. Andrade, S. Menon, and M. Howard. 1994. Continuous administration of anti-interleukin 10 antibodies delays onset of autoimmunity in NZB/W F1 mice. *J. Exp. Med.* 179: 305–310.
42. Cross, J. T., and H. P. Benton. 1999. The roles of interleukin-6 and interleukin-10 in B cell hyperactivity in systemic lupus erythematosus. *Inflamm. Res.* 48: 255–261.
43. Avery, D. T., V. L. Bryant, C. S. Ma, R. de Waal Malefyt, and S. G. Tangye. 2008. IL-21-induced isotype switching to IgG and IgA by human naive B cells is differentially regulated by IL-4. *J. Immunol.* 181: 1767–1779.
44. Wang, X. F., Y. J. Chen, Q. Wang, Y. Ge, Q. Dai, K. F. Yang, Y. H. Fang-Xie, Y. M. Zhou, Y. X. Hu, Mao, and X. G. Zhang. 2007. Distinct expression and inhibitory function of B and T lymphocyte attenuator on human T cells. *Tissue Antigens* 69: 145–153.
45. Perrin, P. J., J. H. Maldonado, T. A. Davis, C. H. June, and M. K. Racke. 1996. CTLA-4 blockade enhances clinical disease and cytokine production during experimental allergic encephalomyelitis. *J. Immunol.* 157: 1333–1336.
46. Butte, M. J., M. E. Keir, T. B. Phamduy, A. H. Sharpe, and G. J. Freeman. 2007. Programmed death-1 ligand 1 interacts specifically with the B7-1 costimulatory molecule to inhibit T cell responses. *Immunity* 27: 111–122.
47. Nakajima, A., M. Azuma, S. Kodera, S. Nuriya, A. Terashi, M. Abe, S. Hirose, T. Shirai, H. Yagita, and K. Okumura. 1995. Preferential dependence of autoantibody production in murine lupus on CD86 costimulatory molecule. *Eur. J. Immunol.* 25: 3060–3069.
48. Hall, A. M., F. J. Ward, C. R. Shen, C. Rowe, L. Bowie, A. Devine, S. J. Urbaniak, C. J. Elson, and R. N. Barker. 2007. Deletion of the dominant autoantigen in NZB mice with autoimmune hemolytic anemia: effects on autoantibody and T-helper responses. *Blood* 110: 4511–4517.
49. Shen, C. R., G. Mazza, F. E. Perry, J. T. Beech, S. J. Thompson, A. Corato, S. Newton, R. N. Barker, and C. J. Elson. 1996. T-helper 1 dominated responses to erythrocyte Band 3 in NZB mice. *Immunology* 89: 195–199.